Tumbling is general

This project is maintained by Julia Lazzari-Dean in the York lab, and was funded by Calico Life Sciences LLC

Research article

From cameras to confocal to cytometry: measuring tumbling rates is a general way to reveal protein binding

Julia R. Lazzari-Dean (ORCID),[*] Austin E.Y.T. Lefebvre, Rebecca Frank Hayward, Lachlan Whitehead, Maria Ingaramo[†], Andrew G. York[‡]

Calico Life Sciences LLC, South San Francisco, CA 94080, USA

[*]*Permanent email: julia.lazzaridean+tumbling@gmail.com*

[†]*Permanent email: maria.del.mar.ingaramo+tumbling@gmail.com*

[‡]*Permanent email: andrew.g.york+tumbling@gmail.com*

Pre-print published: TODO

Please cite as: TODO

Abstract

Molecular interactions are central to understanding any biological system, but they are labor-intensive to measure with most microscopy approaches. Tracking rotational diffusion ("tumbling") offers a generalizable strategy for determining molecular size, from which the presence and size of binding partners can be inferred. However, fluorescence-based tumbling measurements have historically been limited to small targets (<30 kDa) due to the short (nanosecond) lifetime of organic fluorophores and fluorescent proteins. To overcome this size limit, recent studies have explored longer-lived states, such as triggerable triplets, reversibly photoswitched proteins, or

photobleached molecules, opening up a new range of possibilities in tumbling measurements. Here, we develop simulation code to explore the many possible architectures for a tumbling experiment. Using this code, we describe three novel combinations of photophysics and hardware, gearing each to a candidate biological use case. We conclude with experimental tumbling data on a commercial instrument, highlighting the power and accessibility of this approach.

TODO: Lachie animation goes here

Note that this is a limited PDF or print version; animated and interactive figures are disabled. For the full version of this article, please visit TODO: new link https://andrewgyork.github.io/mScarlet_lifetime_reports_pH

Introduction

For 4 billion years, molecular interactions have been essential for life. Each protein, nucleic acid, or lipid in a cell is a character in a chaotic play, zooming from place to place and dancing with different partners to ultimately produce the complex behaviors of living creatures. Mapping out this cascade of interactions is a recurring challenge across biology.

Fluorescence microscopy reveals where molecules are, and with some care, it can also report their abundance [Lakowicz 2006]. Localization is a clue about function, but it's only part of the picture. To understand function, we'd like to monitor the interactions (binding) of our protein of interest in real time in its native context. Unfortunately, fluorescence microscopy is blind to binding information without complicated add-ons, each with considerable downsides (e.g. FRET, FCS, or SPT, discussed in the Appendix).

How might we extract binding information from a generalizable optical readout? Binding changes a molecules' effective size, and different binding partners yield complexes of different overall sizes. Conveniently, the rate of "tumbling," or rotational diffusion, depends on an object's size, with larger objects tumbling more slowly than smaller objects (Figure 2). Therefore, if we can measure tumbling rate, we can report molecular interactions.

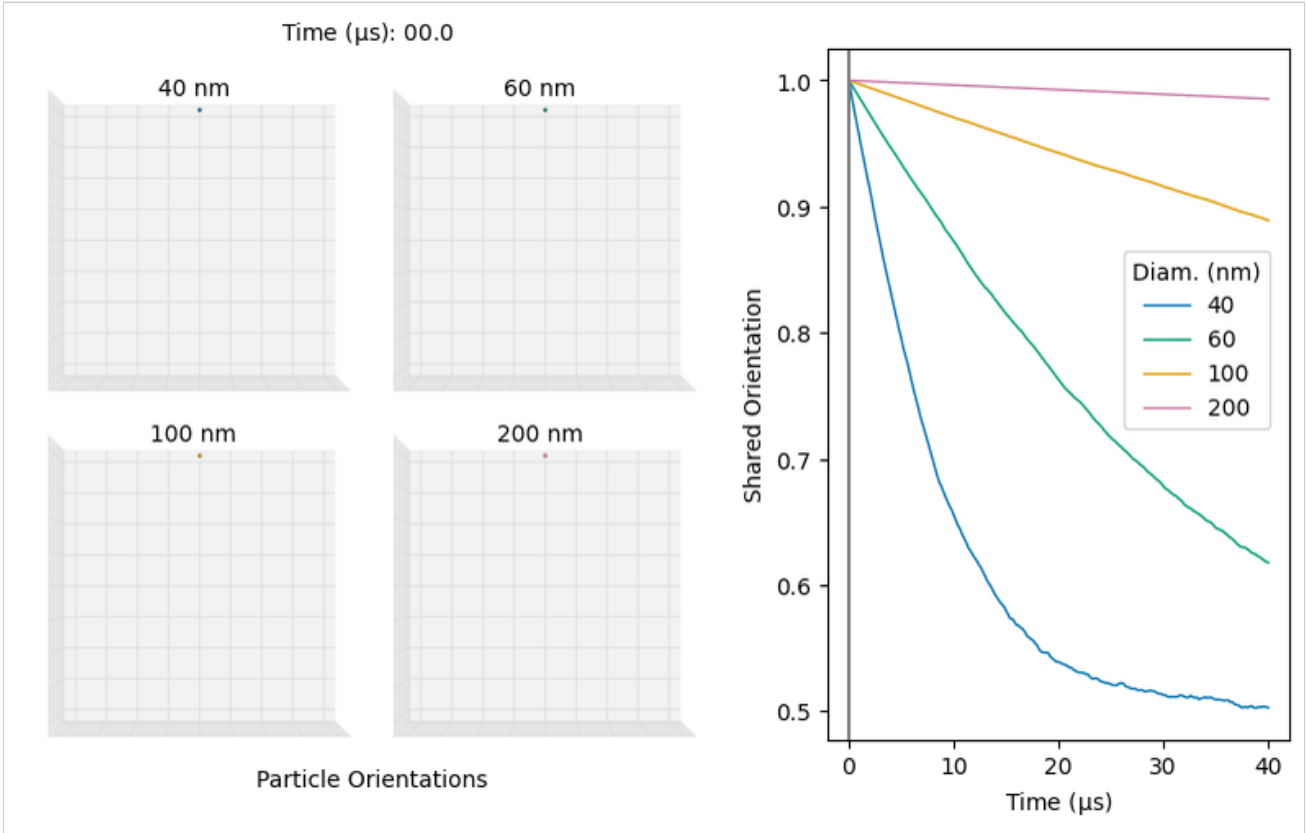

Initial Distribution: North Pole

Figure 2: Scrambling rate of an oriented subset of molecules depends on their size. Simulation of 40, 60, 100, and 200 nm diameter (tumbling times 22, 73, 340, and 2718 µs respectively) decaying from an initial orientation distribution. Points on the sphere represent molecular orientations (analogous to the arrow bouquet diagrams in Figure 1). Shared orientation is quantified as the mean absolute value of the "y" vector component of each particle's orientation. This simulation models diffusive rotation, building on the conceptual rendition in Figure 1. Drop-down options toggle the initial distributions: (1) "north pole", or an artificial initial distribution of axially aligned molecules, (2) a “cap” distribution generated by non-saturating photoselection with linearly polarized light, and (3) a “crescent” pattern as would be generated by (1) followed by a saturating orthogonally polarized depletion beam [York 2019].

The first optical tumbling measurements were based on fluorescence anisotropy [Weber 1952], which reports how much the orientation of a population of fluorophores scrambles during its fluorescence lifetime. To initially generate an oriented population, fluorescence anisotropy takes advantage of "excitation photoselection," which means that fluorophores preferentially absorb polarized light aligned with their absorption dipoles (Figure 1). Following absorption, fluorescence emission typically occurs over a few nanoseconds (the "fluorescence lifetime"), during which tumbling can scramble orientation. The fluorescence emission is polarized along the emission dipole, thereby reporting the total amount of scrambling during those few nanoseconds.

Fluorescence anisotropy allows real-time monitoring of protein binding. Unfortunately, it fails for most proteins, since they are larger than ≈30 kDa and therefore do not tumble detectably during the few-nanosecond fluorescence lifetime. Using the "tumbling" (rotational diffusion) time of GFP (27 kDa=60-90 ns, depending on viscosity [Swaminathan 1997]) and the median size of a eukaryotic protein (50 kDa, [Netzer 1998]), we estimate that the monomers and protein complexes in a cell have tumbling times ranging from 60 ns to a few microseconds. Consider a common cellular event such as assembly and activation of the lysosomal V-ATPase (proton pump). When a single protein component becomes a part of the V1 subunit, we can expect its tumbling time to rise from ≈100 ns to ≈1 μs. This tumbling time would further increase to >>10 μs when the V1 subunit associates with the much larger lysosome to form an active pump [Forgac 1998]. In another example, the 154 kDa lac repressor's tumbling time would increase from ≈300 ns to >10 μs when it binds to DNA and becomes immobilized. At the extreme end of the scale, very large structures, like viral capsids—or beads as in Figure 2—exhibit tumbling times of 10s-100s of microseconds [Volpato 2023].

A powerful but less well-known class of technologies overcomes this size limit by replacing the fluorescence lifetime with long-lived, optically generated states. Since the 1970s, it was recognized that polarized photobleaching can provide information about rotational diffusion and binding [Strackee 1971, Cone 1972, Nigg 1980]. Around the same time, phosphorescence emission was used to record tumbling on the millisecond time scale [Austin 1979, Moore 1979]. These techniques saw some use but were not widely adopted by biologists, in part because of their low signal, phototoxicity, and difficulty in measuring rotation times in the low microseconds.

Recent studies have demonstrated the power of longer-lived, triggerable states to monitor rotational diffusion of protein sizes covering most of the proteome. [Volpato 2023] used the active state of a reversible photoswitchable protein to monitor tumbling over long timescales. Building on this work, [Lu 2023] showed the same principle applies with triggerable fluorescence from a triplet state (termed "optically activated delayed fluorescence"). Beyond just extending the size range, these "triggerable emitters" offer a crucial level of control over the timing of photon production. Unlike previous approaches where photons are emitted spontaneously over a defined lifetime, these states produce photons when triggered, allowing the experimenter to concentrate their limited photon budget into times when it is maximally informative. The value of certain measurement times over others can be seen in Figure 2, where the orientation difference between the 100 and 200 nm beads is much larger at 20 µs than at 2 µs. Thus, triggerable emitters improve both the size range and the signal-to-noise of a tumbling measurement.

The triggerable emitters explored by [Volpato 2023] and [Lu 2023] open up new pulse schemes and hardware configurations ranging far beyond the traditional point-scanning confocal approach typically used for fluorescence anisotropy. This array of possibilities brings its own challenge: identifying the most synergistic combinations of photophysics and hardware. In this work, we first develop open-source tumbling simulation code to explore diverse tumbling architectures. We then simulate tumbling with three different photophysics (photobleaching, rsFPs, triggered triplets) and four hardware configurations (a plate reader, a high throughput imaging system, a cell sorter, and a confocal microscope). We put particular emphasis on pump-probe pulse schemes with triggerable triplets, and we validate their experimental feasibility with data from a commercial confocal microscope. In the future, we envision that tumbling measurements will be possible on most common imaging hardware, as available as red and green color channels are today.

Results and Discussion

Tumbling Simulation Code

We developed numerical simulation code to explore diverse tumbling measurements. We conceptualize tumbling as diffusion on the surface of a sphere, where each point represents a particle's orientation (as shown in Figure 2). We model the diffusion of these points with the numerical approximation described by [Ghosh 2013]. All of the particles in our simulations are

spherical with uniform density, and we assume that viscosity and temperature are held constant. We also assume that all absorption and emission dipoles are parallel.

The simulation tracks each particle's orientation and photophysical state (e.g. ground, excited singlet, triplet) as it tumbles over time. We model two types of state transitions: spontaneous and light-driven. Spontaneous transitions occur from one state to another over time; for example, a fluorescent excited state decays to the ground state with a lifetime of a few nanoseconds. Light-driven transitions are instantaneous in our simulations and occur from one specified state to another; for example, a ground state molecule absorbs light and enters the fluorescent excited state. For light-driven transitions, we choose to specify light intensity in "saturation units," where intensity x excites a fraction of aligned molecules equal to $1-2^{-x}$. A particle's probability of undergoing a light-driven transition also depends on the angle between its orientation (absorption dipole) and the polarization of the incoming light.

Our tumbling simulations share some commonalities. Polarized light excites a population of fluorophores, and their emission is split between two detectors, one that collects light with polarization aligned to the input beam (parallel, $\parallel$) and the other with polarization perpendicular ($\perp$) to the input beam. We choose to represent the relative amounts of these two signals with the polarization, which ranges from 1 (all $\parallel$) to -1 (all $\perp$). Immobile, randomly oriented fluorophores excited with linearly polarized light fluoresce with a polarization of 0.5 (3:1 $\parallel$:$\perp$ ratio) [Lakowicz 2006]. Fluorophores that rotate much faster than the emission fluoresce with polarization≈0. Rates of rotation that are similar to the rate of emission result in polarization between 0 and 0.5.

We suspect that much of the benefit of the simulation code lies in empowering others to use it. In that spirit, we include a short tutorial that simulates fluorescence anisotropy. Furthermore, all of the code to generate the simulations in this work is available on GitHub (TODO: LINK). For faster performance, a GPU-accelerated version is also available.

Simulation 1: Power variation on a plate reader

We first simulate a tumbling measurement with minimal photophysics and hardware. We model a fluorophore that is capable of two photophysical processes: fluorescence emission and photobleaching. When tumbling with photobleaching has been explored in the past, a very fast, very intense polarized light pulse was used to bleach out a subset of the ground state orientations [e.g. Strackee 1971, Cone 1972, Nigg 1980]. The experimenters then used lower

intensity illumination to track the scrambling of this "etched" ground state distribution. This technique requires rapid photobleaching kinetics, high powers, and sub-microsecond detector time resolution, which would be difficult to achieve with low-cost hardware. Here, we take a more minimal, plate-reader compatible approach. We use a single, linearly polarized beam, which continuously illuminates a sample while two detectors integrate polarization of the output fluorescence (Figure 3 with `Photobleaching` selected).

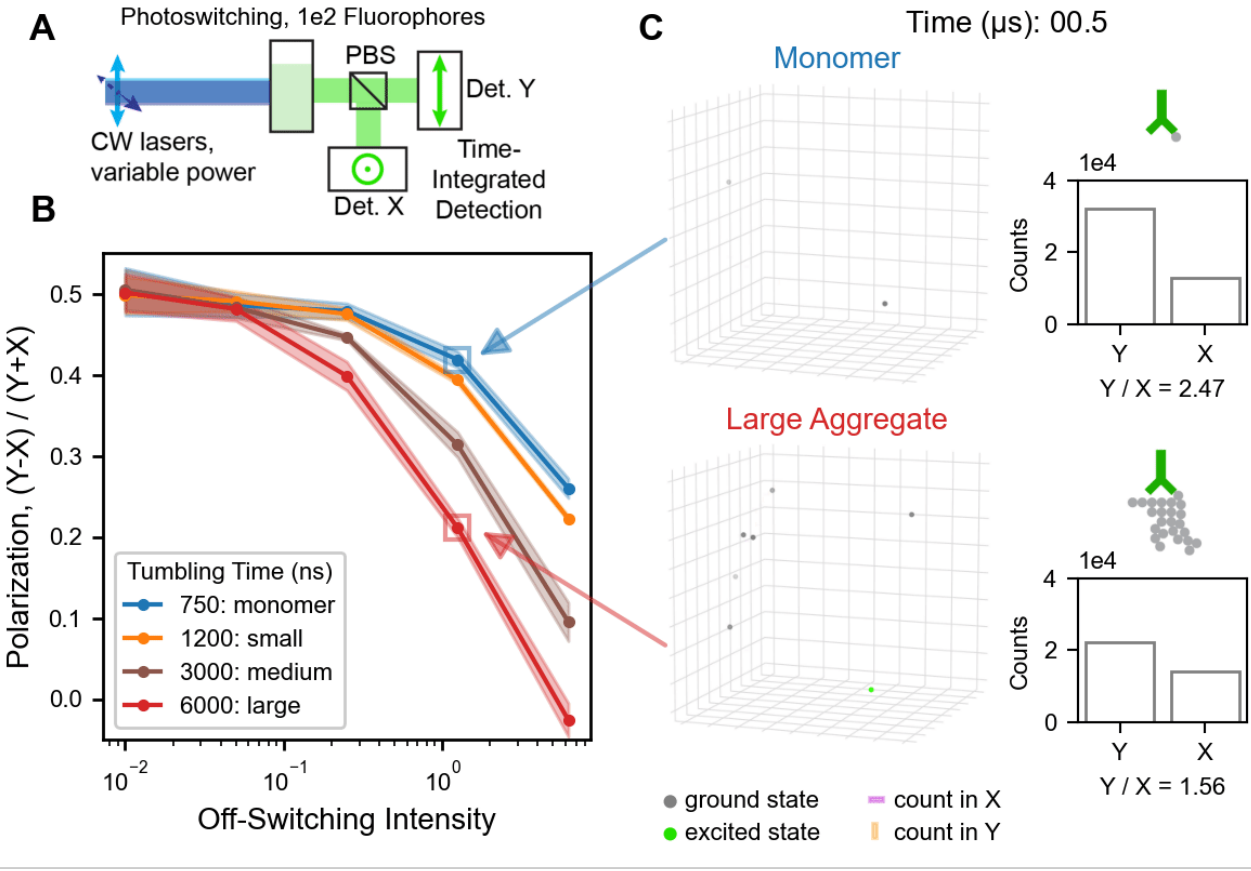

Photophysics: Reversible Photoswitching

Figure 3: Power variations in a photobleaching or off-switching beam reveal size. (A) Cartoon of the simulated experiment, with a laser (light blue) illuminating a bulk solution (e.g. in a cuvette). Two detectors record polarization of the fluorescence emission (green) after a polarizing beam splitter (PBS). For option `Reversible Photoswitching`, an intensity 0.01 on-switching laser (dark blue) was fired concurrently with the off-switching laser (light blue). **(B)** Polarization of the integrated emission signal from the parallel (Y) and perpendicular (X) emission channels as it varies with illumination (Option `Photobleaching`) or off-switching (Option `Reversible Photoswitching`) intensity. Points are means of 3 replicates, with shaded areas indicating ± standard deviation. **(C)** Time course of a measurement with intensity 1.25. Points on a sphere indicate molecular orientations, with the illumination beam oriented in the up/down direction. Bar graphs indicate accumulating signal on the detectors. The slower rotation of the large aggregate increases etching of the ground state orientation (gray) and reduces the polarization.

It is convenient to imagine the time course of this bleaching experiment (Figure 3C, Option `Photobleaching`), even though the final signal can be analyzed in a time-integrated manner. For a fully immobile population, high laser intensity will strongly etch the orientation distribution of the ground state population. Initially, emission will be mostly parallel to the excitation beam, but as bleaching progresses, very few ground state fluorophores will remain parallel to the excitation beam. The remaining fluorophores are mostly perpendicular to the excitation beam, so the detected emissions are more likely to be in the perpendicular channel (lower polarization). Conversely, a population that is rotating rapidly will repopulate the parallel channel and retain high polarization over time, even as the total fluorescence decreases from bleaching. The relative rates of photobleaching and rotation determine the integrated polarization. By varying the laser power one can vary the rate of photobleaching and obtain a spectrum. Although photobleaching is irreversible and destructive to the sample, even a moderate sample volume would be able to diffusively replenish the signal, allowing repeat measurements.

If we allow ourselves to swap out the fluorophore and not rely on photobleaching alone, a reversible photoswitchable fluorescent protein (rsFP) would be an upgrade to the above approach. rsFPs can be switched between an inactive (dark) and an active ground state with different colors of light [Zhou 2013]. Most simply, rsFPs allow 'resetting' to reuse the same molecules for successive measurements. Alternatively, the on- and off-switching lasers could be on simultaneously, thereby regenerating the sample during the measurement (Figure 3 with `Reversible Photoswitching` selected). By varying the power of the off-switching laser, we are tuning the lifetime of the active state. Because these measurements reveal the relative rates of tumbling and some photophysical process, tuning the lifetime of the photophysical process can reveal the tumbling rate and therefore size. We predict that this setup will yield clear signals even for very low numbers of fluorophores (100 total in the simulation).

Our power variation scheme could be applied, for example, with commercially available antibodies in a plate reader to determine level of aggregation of the antibody's target in blood or cerebrospinal fluid. It also could be deployed as an alternative to the common co-immunoprecipitation or "pulldown" assay to determine whether a labeled target protein is bound to any additional molecules in a mixture.

Simulation 2: Spatially resolving binding with triplets

Often, we would like to map the interactions of a protein of interest across a cell or tissue, ideally over a large field of view simultaneously. A standard scientific camera can acquire a snapshot every few milliseconds, but tumbling involves nanosecond- or microsecond-scale dynamics. To obtain the necessary time resolution, tumbling is typically recorded with a fast, single pixel detector [Lakowicz 2006, Volpato 2023, Lu 2023]. Images are then (slowly) formed by raster scanning a point through the sample. Parallelized, multipixel versions of these time-resolved detectors are in development [McShane 2022] but are not yet widely available.

With current detector technology, a “pump-probe” imaging scheme is compelling, in which the time resolution is encoded by a variable delay between pump and probe laser pulses. Each snapshot records a single delay time, and a modest number of points in the tumbling decay curve can be acquired as a series of snapshots at varying delays (Figure 4, left panel). Critically, such an approach would be compatible with widefield imaging or with state-of-the-art lightsheet microscopes [Millett-Sikking 2019].

A pump-probe pulse scheme doesn't discard photons that arrive outside of the "probe" time window; it simply doesn't generate them. To achieve this, we need a long-lived state that can be triggered to emit at a time of interest, such as a reversibly switchable fluorescent protein (rsFPs, discussed above) or a triggered triplet. Triggered triplets (also known as optically activated delayed fluorescence) refers to millisecond-lived triplet states that can emit prompt fluorescence when excited with far-red light [Peng 2021]. Triplets can be generated from the excited singlet, leading to a convenient pulse scheme where a pump pulse at the traditional absorption wavelength (say, 488 nm for fluorescein) is followed by a far-red probe pulse [Demissie 2020]. While we were preparing this manuscript, it was first experimentally reported that the triggered triplet signal is compatible with tumbling measurements [Lu 2023]. Here, we focus on triplets rather than rsFPs because of their superior time flexibility, in principle accessing timescales as short as hundreds of nanoseconds; a more detailed discussion of the advantages and disadvantages of these two options is available in the Appendix.

To explore pump-probe measurements with triggered triplets (Figure 4), we simulated a linearly polarized pump pulse and an orthogonally polarized probe (trigger) pulse. Two gated but otherwise standard cameras record fluorescence following a polarizing beamsplitter. We simulate a sample of labeled protein with three binding states: unbound, bound to a small partner, or bound to a large partner. All three binding states are distinguishable. Importantly, a mixture of the unbound and large states is also distinguishable from a binding partner of

intermediate mass; we anticipate such mixtures will be the norm in a real sample. One could imaging applying this architecture to many biological systems, e.g.:

- Assembly of the multipart protein machines, e.g. the V-ATPase [Forgac 1998]
- Recruitment of downstream effectors of receptor tyrosine kinases to the membrane [Lemmon 2010]
- Transcription factor dimerization and binding to DNA [Amoutzias 2008]

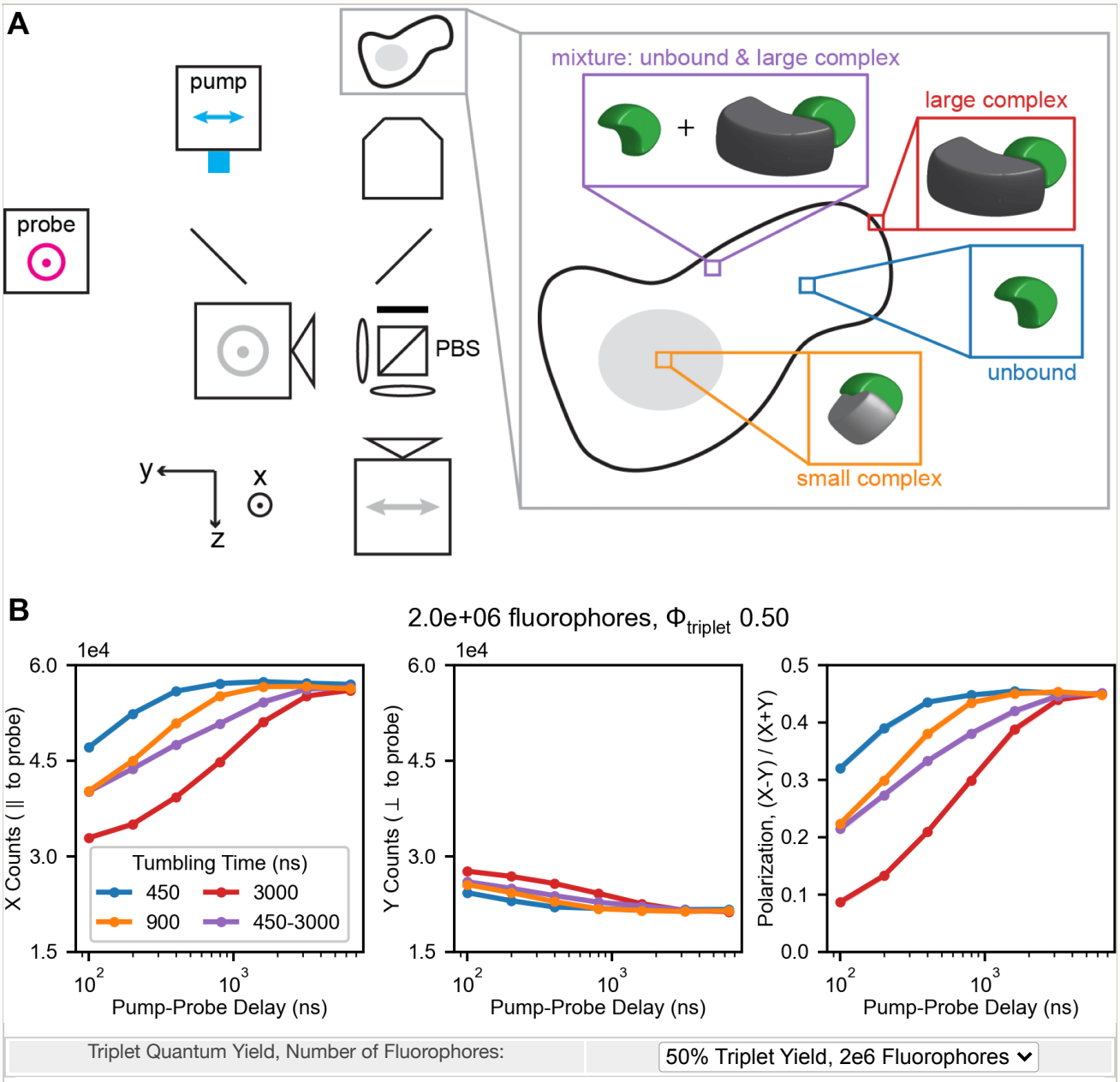

Figure 4. Pump-probe measurements with triggered emitters elucidate spatially resolved binding states. (A) Schematic of a pump-probe measurement with triggered triplets. The pump pulse (blue) generates fluorescence (green) in the sample. Some of these fluorescent molecules convert to triplets (faint pink), which, after a variable delay, are triggered to fluoresce (green) by the probe beam (pink). A fast shutter separates signal from the pump and probe pulses. A polarizing beamsplitter followed by two cameras records the polarized fluorescence at all points in the image. A sequence of delays is captured by successive images. Inset from sample shows a cartoon representation of how tumbling times could correspond to spatially compartmentalized binding events within a cell.

(B) Simulation results for spheres with tumbling times of 450 ("unbound"), 900 ("small complex"), and 3000 ns ("large complex"), as well as an equal part mixture of spheres with 450 and 3000 ns tumbling times. 50 ns pump and probe pulses were simulated as 10 discrete phototransitions of intensity 0.25, each 5 ns apart. Because of the saturating intensity used in these simulations, polarization values deviate from the ideal of 0.5 for fully equilibrated samples. Points indicate means of 6 replicates, with shaded areas indicating ± standard deviation.

The primary drawback of triggered triplets is the low numbers of photons per molecule. The ≈1% quantum yield of triplet generation in existing fluorescent proteins [Peng 2021] is partially responsible for this. More fundamentally, each triplet molecule emits at most one photon on its path to the ground state. To obtain sufficient signal despite this, we simulated a large number of molecules, which can be thought of as either spatially binning the image or acquiring many cycles from the same molecules. In the latter case, the millisecond spontaneous decay of the triplet is advantageous, resetting the sample to its original state for subsequent cycles. The effects of triplet quantum yield and number of molecules on the signal-to-noise ratio can be explored through the drop-down options in Figure 4.

Simulation 3: Recording binding state in high throughput with a flow cytometer

In addition to camera-based recording, pump-probe tumbling schemes enable flow cytometry readouts (Figure 5), dramatically increasing throughput. This throughput opens up the possibility of binding measurements across many conditions, e.g. in large genetic perturbation libraries. Such an approach could characterize the effect of mutagenesis or knockout on protein-protein interactions at scale.

Time delays in a flow setup could be achieved either via physical spacing of the pump and probe laser along the object's path or via time-resolved lasers and detectors. With a linear flow rate of 10 m/s [Kalb 2017], a cell would move 50 μm in 1 μs. Two 10 μm wide laser spots separated by 50 μm would produce a 1 μs delay; a sequence of beam spacings produces a sequence of delays. Flow cytometers often incorporate additional spectral channels in this manner, so this proposal requires minimal modification of existing systems. For time delays shorter than 500 ns, pump-probe pairs could also be delivered within the dwell time of the cell in a particular focused spot, provided that the detector was able to gate out any emission generated by the pump pulse.

A key difference between this approach and a camera-based system (Figure 4) is that it would be inconvenient to wait for milliseconds for untriggered triplets to naturally decay. With flow rates fast enough to achieve microsecond delays, millisecond wait times in between measurements would involve long additional fluidic lines. To allow successive pump-probe sequences without excessive buildup of triplets, we simulate a circularly polarized probe beam (Figure 5 with `Circular` selected), which increases the polarization differences between particle sizes versus using a linearly polarized beam (Figure 5 with `Linear` selected).

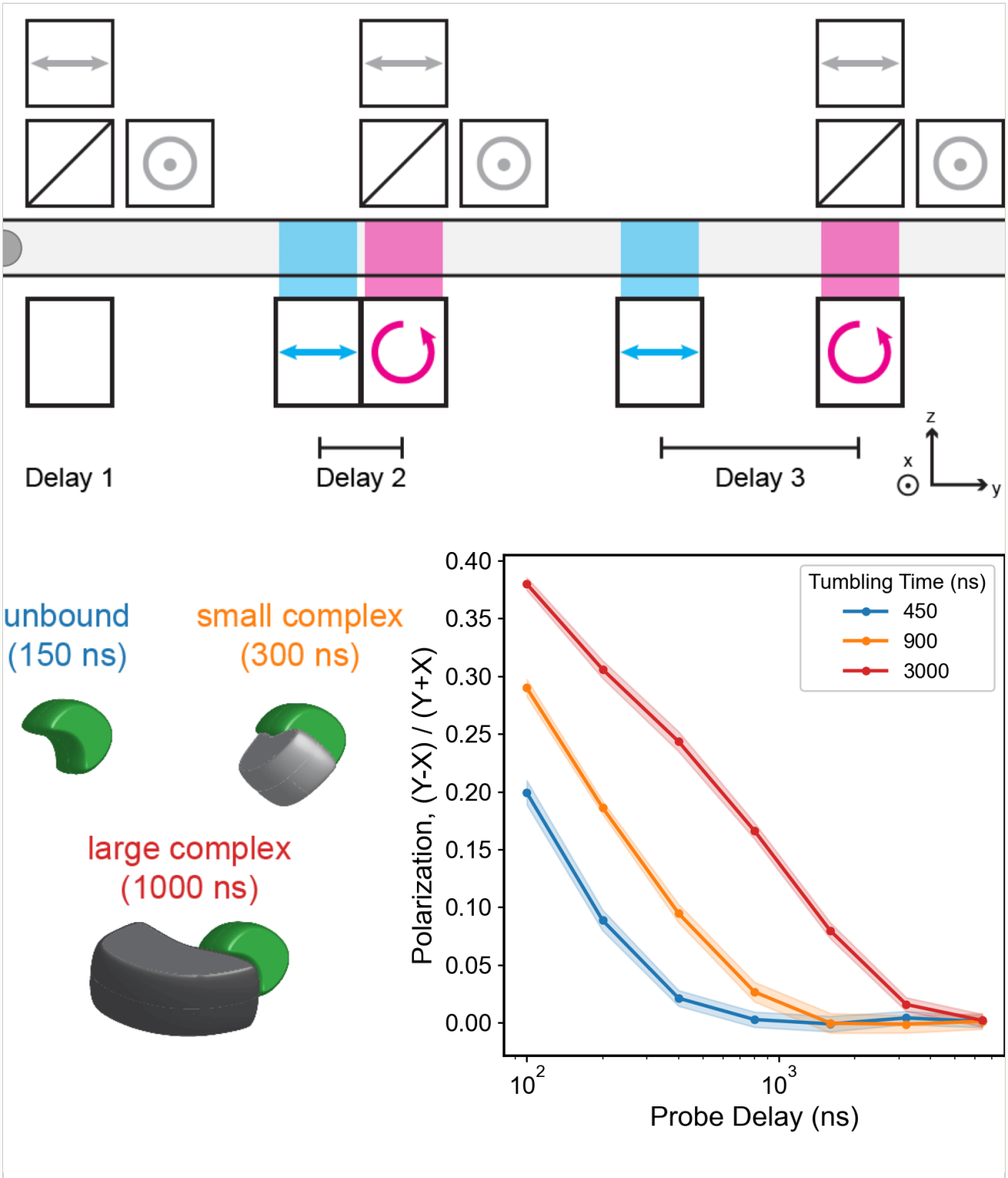

Probe Polarization: Circular (XY plane)

Figure 5. Pump-probe based tumbling measurements are compatible with flow cytometry. Top: Cartoon of a cell in a flow cytometer, interrogated at different tumbling delays as it proceeds through the flow cell. Triggered triplet photophysics are illustrated (green=singlet, pink=triplet), generated by a linearly polarized pump beam (blue) and a circularly (XY plane) or linearly (X) polarized probe beam (pink). A short delay with pulsed pump and probe in one location is shown on the left, with two spatially generated delays with continuous pump and probe illumination in the middle and right. **Bottom left:** Cartoon of how binding states could correspond to rotational diffusion times. **Bottom right:** Simulation results from the described pulse scheme and samples (approximated as spheres). For the purpose of polarization, parallel is defined relative to the pump beam. Points are means of 12 replicate simulations, each with 1e6 molecules and 1% triplet yield. Shaded areas are ± standard deviation. The pink box highlights the decay that the cartoon would be currently measuring.

Experimental demonstration of triggered triplet tumbling

To demonstrate the feasibility of pump probe pulse schemes with triggered triplets, we made a tumbling measurement on our confocal microscope. Although the functionality is not unmasked in software, the necessary hardware exists on certain commercial systems (in this case, Leica SP8, Figure S1). We used linearly polarized illumination to pump fluorophores into the triplet state and orthogonally polarized 775 nm light to confine the triplet population and to trigger triplets to emit. We used successive sweeps of the resonant scanner to interrogate the sample at 60 µs intervals.

To generate fluorescent protein labeled samples at a variety of known sizes, we adsorbed the fluorescent protein mVenus [Kremers 2006] or mScarlet [Bindels 2017] to the surface of carboxyl modified latex beads. We confirmed successful immobilization of the protein and monodispersity of the bead population with time-resolved fluorescence anisotropy (Figure S2) and dynamic light scattering (Figure S3) for all four sizes (40, 60, 100, and 200 nm diameter).

With these samples in hand, we attempted to trigger delayed fluorescence from the triplet state. Consistent with [Peng 2021], we found that low-intensity 775 nm illumination produced fluorescence only if the sample was previously illuminated at 488 nm (mVenus) or 561 nm (mScarlet), suggesting that the initial pulse generated a long-lived triggerable state (i.e. a triplet, Figure S1). mVenus's triplet lifetime was reported to be approximately 1 ms [Peng 2021]; we replicate this and observe a similar triplet lifetime for mScarlet (Figure S4). Following far-red excitation, the triggered fluorescence itself is short-lived, with a lifetime similar to that of the prompt fluorescence from the singlet (≈2 ns, Figure S5, Figure S6). These characteristics are consistent with triggered fluorescence from the triplet state; to our knowledge this is the first report of triplet triggering in a red fluorescent protein (mScarlet).

Most importantly, we then evaluated whether the triggered triplet emission could report bead size (Figure 6). We observe distinct tumbling decays from the 4 bead diameters we explored; these results indicate that the triplet state indeed preserves some orientation information, consistent with [Lu 2023]. Our experimental results also qualitatively match simulations, with similar time dynamics but a reduction in the magnitude of the polarization changes (see Appendix for further discussion).

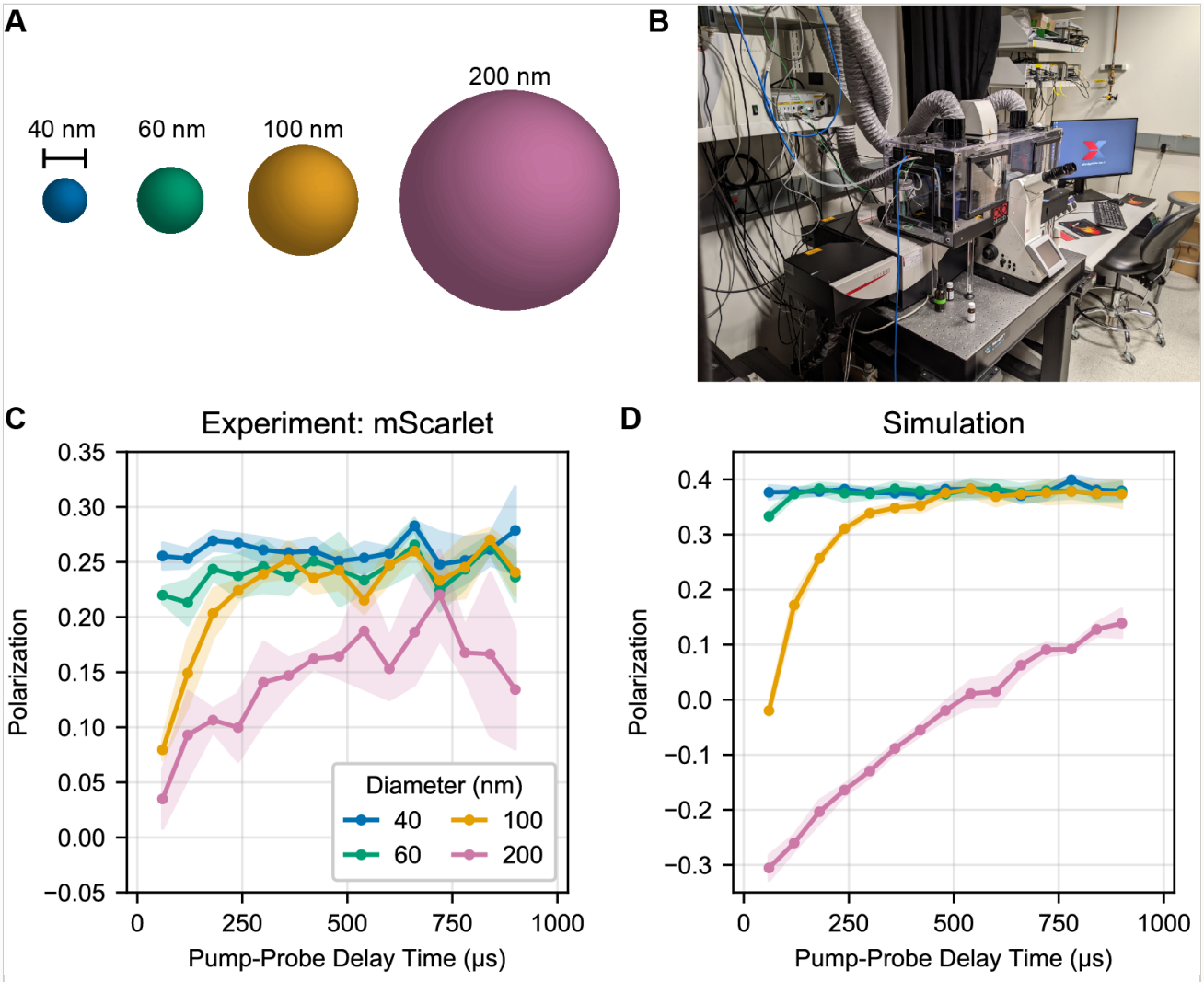

Fluorescent Protein: mScarlet

Figure 6. Tumbling spectroscopy of nanometer-scale beads can be measured on a commercially available microscope with triplet triggering. (A) Cartoon representation of bead samples used in this experiment and simulation. Sample generation is described in the Appendix. **(B)** Photograph of microscope used. Instrumentation scheme is described further in Figure S1. **(C)** Experimental tumbling data acquired on fluorescent-protein labeled beads. Drop-down menu toggles between mScarlet and mVenus recordings. **(D)** Simulation of C with 1e6 molecules and saturating pump (16 pulses of intensity 2) and probe (16 pulses of intensity 0.25) illumination, matching the 200 ns dwell time and 80 MHz repetition rate of the experimental laser. Crescent power was matched to experiment as described in the Appendix. In (C) and (D), points are means, with shaded areas indicating ± standard deviation of n=3 (experiment) or n=6 (simulation) replicates.

Outlook

Determinations of size—and therefore binding—with tumbling are a straightforward and generalizable way to address recurring questions about protein-protein interactions. As discussed in the Appendix, tumbling can in theory outperform existing optical methods for measuring interactions. By tracking rotational diffusion in bulk rather than the translation of single molecules, tumbling measurements are faster and more sensitive than FCS or SPT. By allowing single label measurements without prior structural information, tumbling measurements are a richer and more generalizable binding assay than FRET.

Tumbling can be measured with diverse hardware, making it as attractive in a hand-held or plate-reader format as in a high-resolution imaging system. We have demonstrated that tumbling measurements on nanometer-scale objects are possible with commercially available microscope systems; with software modifications, these measurements could be easy. In addition to a more standard confocal setup, we proposed and simulated tumbling measurements in plate reader, camera-based, and flow cytometry format, each optimized towards protein-protein interaction measurements in a distinct application area. To the best of our knowledge, these systems have not been previously described but would be possible to construct, and our team plans to build in this space in the future.

On the sample side, recent discoveries around "triggerable emitters" or long-lived states with photons on demand [Volpato 2023, Lu 2023] have dramatically expanded the accessible size range and possible signal-to-noise of tumbling measurements. Existing rsFPs and triggerable triplets are an existence proof of triggerable emitters; we anticipate that protein engineering can improve their properties for tumbling applications. For example, high value engineering goals would be fluorescent proteins with higher triplet quantum yields and photoswitchable proteins without intermediate states and dipole rotation [Volpato 2023]. Beyond the fluorophore itself, movement of the label independently from the target (i.e. linker flexibility) can scramble polarization information [Fooksman 2007, Volpato 2023]; improved modular tagging strategies would simplify the onboarding of new proteins of interest.

Most protein-protein interaction assays are confirmatory: the experimenter suspects that two proteins interact and they want to verify this. An idealized tumbling experiment goes far beyond this: it's a discovery engine that, from a single labeled protein, could report the sizes of all

interaction partners, resolved across space and time. Such a tool, when fully realized, will bring us ever closer to understanding the cascades of molecular interactions that underlie life.

Acknowledgements

We thank Andrea Volpato, Ilaria Testa, and Alfred Millett-Sikking for thoughtful advice and feedback. We thank Kayley Hake, Martin Mullis, and Alyssa Kaiser for brainstorming and feedback on the tumbling animation. We thank the many excellent scientists at Calico Life Sciences LLC for providing stimulating discussions throughout this project.

Author Contribution Statement

J.R.L.D. contributed to conceptualization of the project, ran simulations, designed and performed experiments, interpreted data, and wrote the manuscript. A.E.Y.T.L. contributed to conceptualization of the project, ran simulations, and interpreted data. R.F.H. performed experiments. L.W. made the tumbling animation (Figure 1). M.I. performed experiments and contributed to conceptualization of the project. A.G.Y. wrote the fluorophore simulation code and contributed to conceptualization of the project.

Funding and Conflict of Interest Statement

This project was supported by Calico Life Sciences LLC. M.I. and A.G.Y. are inventors on a patent related to tumbling with long-lived states and crescent depletion (US Patent US20210247315A1), and J.R.L.D., M.I., and A.G.Y. have filed a patent on triggered triplets for tumbling.

Open-source software

As always, our work here depends critically on the open-source software community. Among our crucial dependencies (listed with version numbers used in this work):

- Python (version 3.9.9)
- Numpy (version 1.21.4) [Harris 2020]
- Scipy (version 1.7.2) [Virtanen 2020]
- Pandas (version 1.5.3) [pandas-dev 2020]
- Matplotlib (version 3.7.1)
- FFmpeg

We sincerely thank the authors of these projects for enabling our work.

Appendix

Methods and additional discussion can be found in the Appendix, which is also referenced via hyperlinks throughout this article.

References

1. [Lakowicz 2006] Principles of Fluorescence Spectroscopy; J. R. Lakowicz; ISBN 978-0-387-31278-1 (2006) https://doi.org/10.1007/978-0-387-46312-4
2. [York 2019] System and Method for Inferring Protein Binding; A. G. York, M. del Mar Ingaramo; US Patent US20210247315A1 (2019) https://patents.google.com/patent/US20210247315A1/en?oq=WO2019245946A1
3. [Weber 1952] Polarization of the fluorescence of macromolecules. 1. Theory and experimental method; G. Weber; Biochem J., 51, 2, 145–155 (1952) https://doi.org/10.1042/bj0510145
4. [Swaminathan 1997] Photobleaching Recovery and Anisotropy Decay of Green Fluorescent Protein GFP-S65T in Solution and Cells: Cytoplasmic Viscosity Probed by Green Fluorescent Protein Translational and Rotational Diffusion; R. Swaminathan, C. P. Hoang, A. S. Verkman; Biophys J., 72, 4, 1900-7 (1997) https://doi.org/10.1016/S0006-3495(97)78835-0
5. [Netzer 1998] Protein folding in the cytosol: chaperonin-dependent and -independent mechanisms; W. J. Netzer, F. U. Hartl; Trends in Biochemical Sciences, 23, 2, 68-73 (1998) https://doi.org/10.1016/S0968-0004(97)01171-7
6. [Forgac 1998] Structure, function and regulation of the vacuolar (H+)-ATPases; M. Forgac; FEBS Letters, 440, 3, 258-263 (1998) https://doi.org/10.1016/S0014-5793(98)01425-2
7. [Volpato 2023] Extending fluorescence anisotropy to large complexes using reversibly switchable proteins; A. Volpato, D. Ollech, J. Alvelid, M. Damenti, B. Müller, A. G. York, M. Ingaramo, I. Testa; Nature Biotechnology, 41, 552–559 (2023) https://doi.org/10.1038/s41587-022-01489-7
8. [Strackee 1971] Rotational diffusion of rhodopsin-digitonin micelles studied by transient photodichroism; L. Strackee; Biophys. J., 11, 9, 728-38 (1971) https://doi.org/10.1016/S0006-3495(71)86250-1
9. [Cone 1972] Rotational Diffusion of Rhodopsin in the Visual Receptor Membrane; R. A. Cone; Nature New Biology, 236, 39–43 (1972) https://doi.org/10.1038/newbio236039a0

10. [Nigg 1980] Anchorage of a band 3 population at the erythrocyte cytoplasmic membrane surface: Protein rotational diffusion measurements; E. A. Nigg, R. J. Cherry; Proc. Natl. Acad. Sci. USA, 77, 8, 4702-6 (1980) https://doi.org/10.1073/pnas.77.8.4702
11. [Austin 1979] Rotational diffusion of cell surface components by time-resolved phosphorescence anisotropy; R. H. Austin, S. S. Chan, T. M. Jovin; Proceedings of the National Academy of Sciences, 76, 11, 5660-5654 (1979) https://doi.org/10.1073/pnas.76.11.5650
12. [Moore 1979] Phosphorescence depolarization and the measurement of rotational motion of proteins in membranes; C. Moore, D. Boxer, P. Garland; FEBS Letters, 108, 1, 161-166 (1979) https://doi.org/10.1016/0014-5793(79)81200-4
13. [Lu 2023] Sequential Two-Photon Delayed Fluorescence Anisotropy for Macromolecular Size Determination; Y.-H. Lu, M. C. Jenkins, K. G. Richardson, S. Palui, M. S. Islam, J. Tripathy, M. G. Finn, R. M. Dickson; J. Phys. Chem. B, 127, 17, 3861–3869 (2023) https://doi.org/10.1021/acs.jpcb.3c01236
14. [Ghosh 2013] A "Gaussian" for diffusion on the sphere; A. Ghosh, J. Samuel, arXiv:1303.1278v1 (2013) https://doi.org/10.48550/arXiv.1303.1278
15. [Zhou 2013] Photoswitchable Fluorescent Proteins: Ten Years of Colorful Chemistry and Exciting Applications; X. X. Zhou, M. Z. Lin, 17, 4, 682–690. (2013) https://doi.org/10.1016/j.cbpa.2013.05.031
16. [McShane 2022] High resolution TCSPC imaging of diffuse light with a one-dimensional SPAD array scanning system; AE. P. McShane, H. K. Chandrasekharan, A. Kufcsák, N. Finlayson, A. T. Erdogan, R. K. Henderson, K. Dhaliwal, R. R. Thomson, M. G. Tanner; Optics Express, 30, 15, 27926-27937 (2022) https://doi.org/10.1364/OE.461334
17. [Millett-Sikking 2019] High NA single-objective light-sheet; A. Millett-Sikking, K. M. Dean, R. Fiolka, A. Fardad, L. Whitehead, A. G. York; Zenodo. (2019) https://doi.org/10.5281/zenodo.3244420
18. [Peng 2021] Optically Modulated and Optically Activated Delayed Fluorescent Proteins through Dark State Engineering; B. Peng, R. Dikdan, S. E. Hill, A. C. Patterson-Orazem, R. L. Lieberman, C. J. Fahrni, R. M. Dickson; J Phys Chem B, 125, 20, 5200-5209 (2021) https://doi.org/10.1021/acs.jpcb.1c00649
19. [Demissie 2020] Triplet Shelving in Fluorescein and Its Derivatives Provides Delayed, Background-Free Fluorescence Detection; A. A. Demissie, R. M. Dickson; J Phys Chem A 124, 7, 1437-1443 (2020) https://doi.org/10.1021/acs.jpca.9b11040
20. [Lemmon 2010] Cell signaling by receptor-tyrosine kinases; M. A. Lemmon, J. Schlessinger; Cell, 141, 7, 1117–1134 (2010) https://doi.org/10.1016/j.cell.2010.06.011

21. [Amoutzias 2008] Choose your partners: dimerization in eukaryotic transcription factors; G. D. Amoutzias, D. L. Robertson, Y. Van de Peer, S. G. Oliver; Trends in Biochemical Sciences, 33, 5, 220-229 (2008) https://doi.org/10.1016/j.tibs.2008.02.002
22. [Kalb 2017] Line Focused Optical Excitation of Parallel Acoustic Focused Sample Streams for High Volumetric and Analytical Rate Flow Cytometry; D. M. Kalb, F. A. Fencl, T. A. Woods, A. Swanson, G. C. Maestas, J. J. Juárez, B. S. Edwards, A. P. Shreve, S. W. Graves; Anal. Chem., 89, 18, 9967-9975 (2017) https://doi.org/10.1021/acs.analchem.7b02319
23. [Kremers 2006] Cyan and Yellow Super Fluorescent Proteins with Improved Brightness, Protein Folding, and FRET Förster Radius; G.-J. Kremers, J. Goedhart, E. B. van Munster, T. W. J. Gadella; Biochemistry, 45, 21, 6570-6580 (2006) http://doi.org/10.1021/bi0516273
24. [Bindels 2017] mScarlet: a bright monomeric red fluorescent protein for cellular imaging; D. S. Bindels, L. Haarbosch, L. van Weeren, M. Postma, K. E. Wiese, M. Mastop, S. Aumonier, G. Gotthard, A. Royant, M. A. Hink, T. W. J. Gadella Jr; Nature Methods 14, 53-56 (2017) http://doi.org/10.1038/nmeth.4074
25. [Fooksman 2007] Measuring Rotational Diffusion of MHC Class I on Live Cells by Polarized FPR; D. R. Fooksman, M. Edidin, B. G. Barisas; Biophys Chem, 130, 1-2, 10-16 (2007) https://doi.org/10.1016/j.bpc.2007.06.013
26. [Harris 2020] Array programming with NumPy; Charles R. Harris, K. Jarrod Millman, Stéfan J. van der Walt, Ralf Gommers, Pauli Virtanen, David Cournapeau, Eric Wieser, Julian Taylor, Sebastian Berg, Nathaniel J. Smith, Robert Kern, Matti Picus, Stephan Hoyer, Marten H. van Kerkwijk, Matthew Brett, Allan Haldane, Jaime Fernández del Río, Mark Wiebe, Pearu Peterson, Pierre Gérard-Marchant, Kevin Sheppard, Tyler Reddy, Warren Weckesser, Hameer Abbasi, Christoph Gohlke & Travis E. Oliphant; Nature 585, 357–362 (2020) http://doi.org/10.1038/s41586-020-2649-2
27. [Virtanen 2020] SciPy 1.0: Fundamental Algorithms for Scientific Computing in Python; Pauli Virtanen, Ralf Gommers, Travis E. Oliphant, Matt Haberland, Tyler Reddy, David Cournapeau, Evgeni Burovski, Pearu Peterson, Warren Weckesser, Jonathan Bright, Stéfan J. van der Walt, Matthew Brett, Joshua Wilson, K. Jarrod Millman, Nikolay Mayorov, Andrew R. J. Nelson, Eric Jones, Robert Kern, Eric Larson, CJ Carey, İlhan Polat, Yu Feng, Eric W. Moore, Jake VanderPlas, Denis Laxalde, Josef Perktold, Robert Cimrman, Ian Henriksen, E.A. Quintero, Charles R Harris, Anne M. Archibald, Antônio H. Ribeiro, Fabian Pedregosa, Paul van Mulbregt, and SciPy 1.0 Contributors; Nature Methods, 17(3) 261-272 (2020) http://doi.org/10.1038/s41592-019-0686-2
28. [pandas-dev 2020] pandas-dev/pandas: Pandas; The pandas development team; Zenodo (2020) http://doi.org/10.5281/zenodo.3509134

Hosted on

GitHub Pages